

Amortized Inference and Learning in Latent Conditional Random Fields for Weakly-Supervised Semantic Image Segmentation

Gaurav Pandey Ambedkar Dukkipati
 Indian Institute of Science
 Bangalore

{gaurav.pandey, ad}@csa.iisc.ernet.in

Abstract

Conditional random fields (CRFs) are commonly employed as a post-processing tool for image segmentation tasks. The unary potentials of the CRF are often learnt independently by a classifier, thereby decoupling the inference in CRF from the training of classifier. Such a scheme works effectively, when pixel-level labelling is available for all the images. However, in absence of pixel-level labels, the classifier is faced with the uphill task of selectively assigning the image-level labels to the pixels of the image. Prior work often relied on localization cues, such as saliency maps, objectness priors, bounding boxes etc., to address this challenging problem. In contrast, we model the labels of the pixels as latent variables of a CRF. The pixels and the image-level labels are the observed variables of the latent CRF. We amortize the cost of inference in the latent CRF over the entire dataset, by training an inference network to approximate the posterior distribution of the latent variables given the observed variables. The inference network can be trained in an end-to-end fashion, and requires no localization cues for training. Moreover, unlike other approaches for weakly-supervised segmentation, the proposed model doesn't require further post-processing. The proposed model achieves performance comparable with other approaches that employ saliency masks for the task of weakly-supervised semantic image segmentation on the challenging VOC 2012 dataset.

1. Introduction

Conditional random fields (CRF) are discriminative graphical models, commonly employed for modelling data with structured output. Subsequent to their introduction in 2001 [16], CRFs have been widely used for applications in text processing and computer vision. These include, but are not limited to, image segmentation [7], named entity recognition [30] and POS tagging [25].

Prior to 2014, CRFs were ubiquitously employed for addressing the challenging problem of semantic image segmentation [7, 32, 15, 26, 33, 10, 13, 40], where the goal is to assign a label to each pixel of an image. However, the success of deep learning in computer vision [14, 6] has shifted the focus to fully convolutional neural networks (CNN) for training semantic segmentation models [18], while CRFs have been sublet the task of post-processing the segmentation masks during inference [2, 3, 21, 20, 41].

Hence, most successful models for semantic image segmentation employ some variation of CNN for computing the probability distribution over the classes for each pixel. During inference, these distributions are fed as unary potentials to a fully connected CRF with Gaussian edge potentials, and a joint labeling for the pixels of the image is inferred from the CRF. The work by Krähenbühl & Koltun [13], allows for efficient inference in such models.

Due to the expressive power of CNN, it is theoretically possible to learn segmentation masks without involving a CRF during training. This is especially true, if one has access to a large number of images that have been densely labelled. However, as has been observed by several other researchers [21, 24, 23], dense labeling of images is an expensive and time-consuming operation. The number of densely labeled images form a minuscule percentage of the total set of available labeled images. Hence, the models that rely solely on densely labeled images, are limited in their scope, due to the availability of the data. These models will be referred to as fully-supervised models in the sequel.

The limitations of fully supervised models has necessitated the development of models that can incorporate weakly labeled images for training. These include models that utilize bounding box prior [17, 4, 21, 39], few points per class [1] and image-level labels [38, 34, 21, 24, 23, 22, 31, 28, 35]. Of particular interest are models that rely on image-level labels only, since the web provides an almost unlimited source of annotated images.

Unfortunately, the decoupled CNN-CRF combination (or CNN alone) fares poorly, when only image-level la-

bels are available, as has been observed by several researchers in the past [24, 22]. To alleviate this hurdle, several researchers have resorted to the use of localization cues, such as saliency and attentions maps [37, 11] or objectness priors [24, 36], thereby improving performance to an extent. Improvements in CNN architecture for segmentation [3, 41], has further aided in improved performance.

In this paper, we aim to shift the focus from localization cues and network architecture to conditional random fields for weakly supervised semantic segmentation. In particular, we model the pixel-level labels as the latent features of a conditional random field, while the pixels of the image and the image-level labels form the observed features. The pairwise potentials of the CRF are defined as in [13]. Given the pixels of the image and global label for each image, the aim is to infer the distribution of the latent features for all the images.

One of the major hurdles in employing a CRF with CNN during training, is the cost of exact inference in such a model. In recent years, this issue has been addressed by unrolling few iterations of the mean-field updates of CRF, either implicitly [12, 29], or explicitly as layers of an RNN [42]. This increases the cost of training by a factor proportional to the number of unrolled iterations.

In this paper, we use variational inference to compute a posterior over the latent features (pixel-level labels), as well. However, rather than optimizing the approximate posterior for each example separately, we amortize the cost of inference over the entire dataset. Specifically, we train a CNN that takes the image as input to model the posterior distribution over the corresponding pixel-level labels. This reduces the cost of training as well as inference, since the inference network is a single CNN module. It is important to point out that the proposed model doesn't learn the unary potentials of the CRF, which is the aim in [12, 29]. Rather, we train the inference network to output pixel-level labels that are globally consistent with the image-level label and locally consistent with each other.

Compared with networks that use only global consistency (image-level classification error) for weakly-supervised segmentation [21, 22, 24], the proposed model results in a tremendous improvement in performance, while utilizing a similar architecture. Moreover, we were also able to achieve performance comparable with other networks that employ localization cues, such as saliency and attention maps for training, for the task of weakly-supervised semantic segmentation on VOC 2012 dataset.

2. The proposed model

Let $\mathbf{x}^{(i)}$, $1 \leq i \leq n$ be n images and $\mathbf{y}^{(i)}$, $1 \leq i \leq n$ be the corresponding image-level labels. Each $\mathbf{y}^{(i)}$ is a boolean vector whose length equals the number of classes used for training. Moreover, let $\mathbf{z}^{(i)} = (z_j^{(i)}, 1 \leq j \leq m)$, $1 \leq i \leq$

n be the corresponding pixel-level labels. Note that we use one-hot encoding for $z_j^{(i)}$, that is, $z_j^{(i)} = (0, 0, 1, 0, 0)$, if the j^{th} pixel in i^{th} image is assigned to the third class, and the total number of classes is 5. We will use the phrase pixel-level labels and segmentation masks interchangeably in the sequel. Given $(\mathbf{x}^{(i)}, \mathbf{y}^{(i)})$, $1 \leq i \leq n$, we wish to learn a smooth mapping from $\mathbf{x}^{(i)}$ to $\mathbf{y}^{(i)}$, that allows inference of the pixel-level labels $\mathbf{z}^{(i)}$.

The conditional distribution of the image-level labels \mathbf{y} given the image \mathbf{x} can be written in the following form:

$$p(\mathbf{y}|\mathbf{x}) = \sum_{\mathbf{z}} p(\mathbf{z}|\mathbf{x})p(\mathbf{y}|\mathbf{z}, \mathbf{x}) \quad (1)$$

The aim is to maximize $\sum_{i=1}^n \log p(\mathbf{y}^{(i)}|\mathbf{x}^{(i)})$ for $1 \leq i \leq n$.

Towards that end, we define the conditional distribution of the latent features \mathbf{z} given \mathbf{x} as a pairwise CRF as below:

$$p(\mathbf{z}|\mathbf{x}) \propto \exp \left(- \sum_{j < j'} \psi_{j,j'}(z_j, z_{j'}; \mathbf{x}) \right), \quad (2)$$

where $\psi_{j,j'}(z_j, z_{j'}; \mathbf{x}) = k(\mathbf{t}_j, \mathbf{t}_{j'})\mu(z_j, z_{j'})$. Here, \mathbf{t}_j is the feature vector at location j and $\mu(j, j')$ is the compatibility between the labels z_j and $z_{j'}$. For this work, we follow the definition of feature vectors and kernel potentials as used in [13], that is,

$$k(\mathbf{t}_j, \mathbf{t}_{j'}) = w^{(1)} \exp \left(- \frac{|l_j - l_{j'}|^2}{2\theta_\alpha^2} - \frac{|x_j - x_{j'}|^2}{2\theta_\beta^2} \right) + w^{(2)} \exp \left(- \frac{|l_j - l_{j'}|^2}{2\theta_\gamma^2} \right), \quad (3)$$

where l_j are the x, y coordinates, and x_j is the RGB intensity at location j .

The distribution $p(\mathbf{z}|\mathbf{x})$ serves as a prior distribution over the segmentation mask and encourages the segmentation mask to incorporate information about the brightness and location of the corresponding pixels. Note that, $p(\mathbf{z}|\mathbf{x})$ has no trainable parameters. This was explicitly done, since learning the parameters of a CRF is computationally expensive. Instead, we parametrize the distribution $p(\mathbf{y}|\mathbf{z}, \mathbf{x})$ to serve a similar task as the unary potentials of the CRF.

In particular, we assume that the distribution over the image-level labels factorizes, that is,

$$p(\mathbf{y}|\mathbf{z}, \mathbf{x}) = \prod_{k=1}^K p(y_k|\mathbf{z}, \mathbf{x}), \quad (4)$$

where K is the number of classes and y_k is a binary random variable indicating whether the k^{th} class is present or absent in the image. The probability of y_k being 1 is given by:

$$p(y_k = 1|\mathbf{z}, \mathbf{x}) = \frac{\sum_{j=1}^m z_{jk} \phi_{jk}(\mathbf{x})}{1 + \sum_{j=1}^m \phi_{jk}(\mathbf{x})} \quad (5)$$

An EM algorithm to train ϕ , would proceed by generating samples from $p(\mathbf{z}|\mathbf{x}, \mathbf{y})$, fix those samples, and then maximize $\log p(\mathbf{y}|\mathbf{z}, \mathbf{x})$ using those samples (since $p(\mathbf{z}|\mathbf{x})$ has no trainable parameters). Unfortunately, sampling from $p(\mathbf{z}|\mathbf{x}, \mathbf{y})$ is computationally intractable. Hence, we resort to a variational approach for optimizing $p(\mathbf{y}|\mathbf{x})$.

2.1. The lower bound

We introduce a variational distribution $q(\mathbf{z}|\mathbf{x}, \mathbf{y})$, and obtain a lower bound on the conditional log-likelihood as follows:

$$\log p(\mathbf{y}|\mathbf{x}) = \log \sum_{\mathbf{z}} p(\mathbf{z}|\mathbf{x})p(\mathbf{y}|\mathbf{z}, \mathbf{x}) \quad (6)$$

$$= \log \sum_{\mathbf{z}} q(\mathbf{z}|\mathbf{y}, \mathbf{x}) \frac{p(\mathbf{y}|\mathbf{z}, \mathbf{x})p(\mathbf{z}|\mathbf{x})}{q(\mathbf{z}|\mathbf{y}, \mathbf{x})} \quad (7)$$

$$\geq \sum_{\mathbf{z}} q(\mathbf{z}|\mathbf{y}, \mathbf{x}) \log \frac{p(\mathbf{y}|\mathbf{z}, \mathbf{x})p(\mathbf{z}|\mathbf{x})}{q(\mathbf{z}|\mathbf{y}, \mathbf{x})} \quad (8)$$

$$= -\text{KL}(q(\mathbf{z}|\mathbf{y}, \mathbf{x})||p(\mathbf{z}|\mathbf{x})) + \mathbb{E}_{q(\mathbf{z}|\mathbf{x}, \mathbf{y})} \log p(\mathbf{y}|\mathbf{z}, \mathbf{x}), \quad (9)$$

where the inequality in the lower bound appears due to Jensen’s inequality.

The first term in (9) forces the variational distribution q to be ‘close’ to the prior distribution for the image \mathbf{x} , that is, $p(\mathbf{z}|\mathbf{x})$. This forces q to generate fine-grained segmentation masks that take into account pixel brightness and location. The second term trains the variational distribution to generate segmentation masks that improve classification performance.

In this work, we assume that the variational distribution q factorizes completely, that is

$$q(\mathbf{z}|\mathbf{x}, \mathbf{y}) = \prod_{j=1}^m q(z_j|\mathbf{y}, \mathbf{x}) \quad (10)$$

Moreover,

$$q(z_{jk} = 1|\mathbf{x}, \mathbf{y}) = \frac{\exp(g_{jk}(\mathbf{x}))}{\sum_{k'=1}^K \exp(g_{jk'}(\mathbf{x}))} \equiv \varphi_{jk}(\mathbf{x}), \quad (11)$$

where g is a fully convolutional neural network and $\{g_{jk}(\mathbf{x}), 1 \leq j \leq m, 1 \leq k \leq K\}$, are the outputs of g , when \mathbf{x} is fed as input. The architecture of the CNN used is discussed in the experiments section. The CNN g will be referred to as the inference network in the sequel. Note that we don’t explicitly model the variational distribution q as a function of \mathbf{y} , since \mathbf{y} wouldn’t be available for the test data. We will denote $q(z_{jk} = 1|\mathbf{x}, \mathbf{y})$ as $\varphi_{jk}(\mathbf{x})$.

2.2. Training the inference network

In this section, the training of the inference network g with respect to the objective function (9) will be discussed.

In particular, the gradient of the objective function with respect to $\varphi_{jk}(\mathbf{x})$ will be derived. The gradient with respect to the parameters of CNN g can then be computed via back-propagation.

The KL-divergence term in (9) can be rewritten as:

$$-\text{KL}(q(\mathbf{z}|\mathbf{y}, \mathbf{x})) = \mathcal{H}(q(\mathbf{z}|\mathbf{y}, \mathbf{x})) - \sum_{j < j'} k(\mathbf{t}_j, \mathbf{t}_{j'}) \mathbb{E}_{q(z_j, z_{j'}|\mathbf{y}, \mathbf{x})} \mu(z_j, z_{j'})$$

Differentiating the above with respect to $\varphi_{jk}(\mathbf{x})$, we get

$$-\nabla_{\varphi_{jk}(\mathbf{x})} \text{KL} = -1 - \log(\varphi_{jk}(\mathbf{x})) - \sum_{j' \neq j} k(\mathbf{t}_j, \mathbf{t}_{j'}) \sum_{k'=1}^K \varphi_{j'k'}(\mathbf{x}) \mu(z_j, z_{j'}) \quad (12)$$

An efficient algorithm for computing the above quantity using permutohedral lattice has been discussed in [13]. Note that, we need to compute the above quantity only once for computing the exact gradient. This is in contrast with standard mean-field approaches that require similar computations to proceed till convergence.

Exact computation of the gradient of the second term in (9) with respect to $\varphi_{jk}(\mathbf{x})$ is intractable. One possible solution is to approximate the gradient by generating samples from $q(\mathbf{z}|\mathbf{x}, \mathbf{y})$. Note that, $q(\mathbf{z}|\mathbf{x}, \mathbf{y})$ is a fully-factorized distribution and hence, sampling can be done in parallel very efficiently. The gradient of the second term can then be rewritten as:

$$\begin{aligned} \nabla \mathbb{E}_{q(\mathbf{z}|\mathbf{x}, \mathbf{y})} \log p(\mathbf{y}|\mathbf{z}, \mathbf{x}) &= \mathbb{E}_{q(\mathbf{z}|\mathbf{x}, \mathbf{y})} \nabla \log q(\mathbf{z}|\mathbf{x}, \mathbf{y}) \log p(\mathbf{y}|\mathbf{z}, \mathbf{x}) \\ &\approx \sum_{l=1}^L \nabla \log q(\mathbf{z}^{(l)}|\mathbf{x}, \mathbf{y}) \log p(\mathbf{y}|\mathbf{z}^{(l)}, \mathbf{x}) \end{aligned} \quad (13)$$

However, we found that the resultant gradients had high variance. Therefore, we approximated the multinomial distribution $q(z_j|\mathbf{x}, \mathbf{y})$ by its continuous relaxation $q_\pi(z_j|\mathbf{x}, \mathbf{y})$. This distribution is known as the concrete distribution or Gumbel-softmax distribution [8, 19].

A sample $\bar{z}_j = (\bar{z}_{j1}, \dots, \bar{z}_{jK})$ from the continuous relaxation $q_\pi(z_j|\mathbf{x}, \mathbf{y})$ has the following form:

$$\bar{z}_{jk} = \frac{\exp((\log \varphi_{jk}(\mathbf{x}) + \gamma_{jk})/\tau)}{\sum_{k'=1}^K \exp((\log \varphi_{jk'}(\mathbf{x}) + \gamma_{jk'})/\tau)} \quad (14)$$

where τ is the temperature that performs trade off between the variance of the samples and accuracy of the updates. Moreover, $\gamma_{jk}, 1 \leq k \leq K$ are *i.i.d* samples from the Gumbel distribution (denoted as G in the sequel), and can be sampled as $\gamma_{jk} = -\log(-\log(U)), U \sim \text{Uniform}[0, 1]$. To

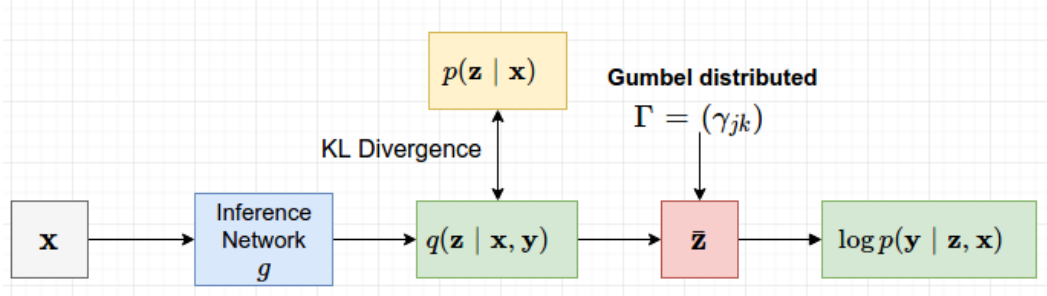


Figure 1: Representation of the implemented model. The image \mathbf{x} is fed to the inference network to compute the parameters of the variational distribution q . The KL-divergence between q and $p(\mathbf{z}|\mathbf{x})$ is minimized and the corresponding derivative backpropagated. Next, samples from the Gumbel-softmax approximation are generated and fed to the classification network. The gradient of the network is computed with respect to the relaxed sample and backpropagated.

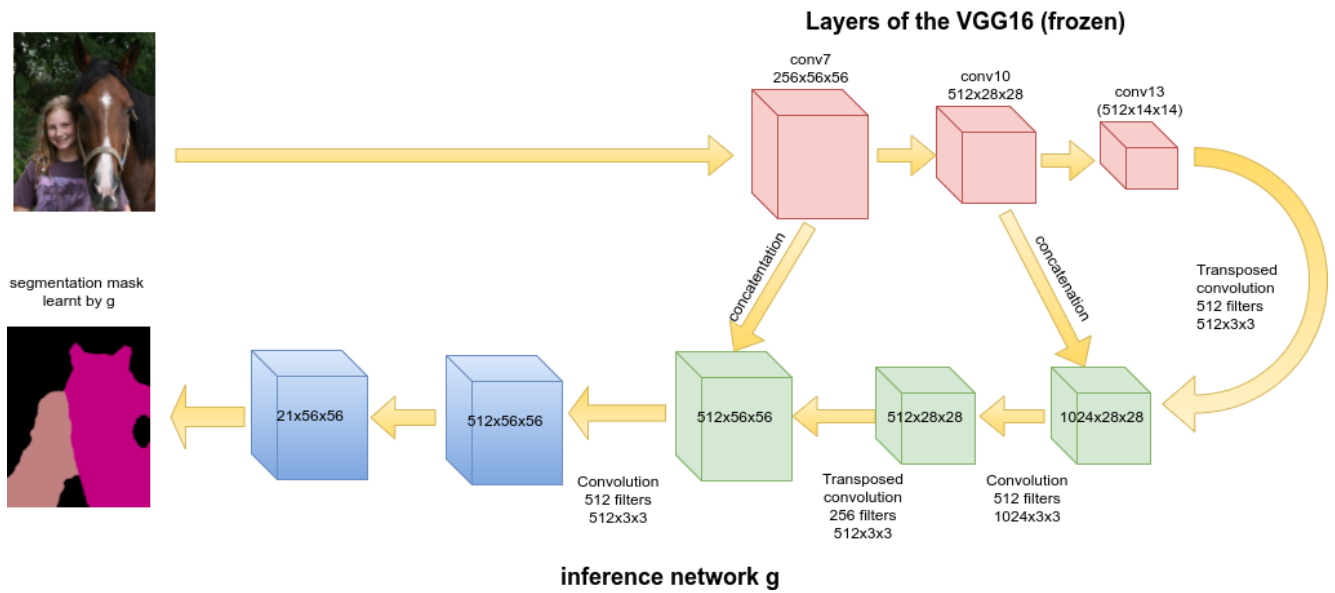


Figure 2: The inference network of the proposed model. Except for the last layer, each convolutional layer in the inference network is followed by a ReLU layer and a batch normalization layer. The last layer is followed by exponentiation and normalization to get ϕ .

know more about Gumbel-softmax distribution, the reader is encouraged to refer to [8].

Using the above approximation, the samples $\bar{\mathbf{z}}$ from $q(\mathbf{z}|\mathbf{y}, \mathbf{x})$ can be expressed as a continuous function of the parameters of the network g . Hence, the gradient of the second term in (9) with respect to $\varphi_{jk}(\mathbf{x})$ can be rewritten as:

$$\begin{aligned} \nabla_{\varphi_{jk}(\mathbf{x})} \mathbb{E}_{q(\mathbf{z}|\mathbf{x}, \mathbf{y})} \log p(\mathbf{y}|\mathbf{z}, \mathbf{x}) \\ = \mathbb{E}_{\Gamma \sim G} \nabla_{\varphi_{jk}(\mathbf{x})} \log p(\mathbf{y}|\bar{\mathbf{z}}, \mathbf{x}), \end{aligned} \quad (15)$$

where $\Gamma = (\gamma_{jk})$ and $\bar{\mathbf{z}} = (\bar{z}_{jk})$. Moreover, \bar{z}_{jk} is a function of $\varphi_{jk}(\mathbf{x})$ and γ_{jk} as defined in (14). Since $\log p(\mathbf{y}|\bar{\mathbf{z}}, \mathbf{x})$ is a differentiable function of $\bar{\mathbf{z}}$, the gradient can be computed using chain rule.

2.3. Implementation details

We use minibatch training to learn the parameters of the model, whereby the gradient of the model with respect to the parameters of the inference network g are computed for every minibatch and the corresponding parameters updated. While the gradient of the KL-divergence can be computed exactly from (12), the gradient of the classification error in (15) requires one to sample Gumbel-distributed random variables. In practice, when the minibatch size is large enough, it is sufficient to sample one Gumbel random variable for each z_{jk} . per training example, and then compute the gradient of the classification error with respect to the parameters, for this vector. This has also been observed for the case of variational autoencoder in [9].

We don't perform any explicit training of function ϕ from equation (5). Instead, we define ϕ_{jk} as follows:

$$\phi_{jk}(\mathbf{x}) = d^{l_j}, \quad (16)$$

where l_j is the rank of $\varphi_{jk}(\mathbf{x})$, when the list $(\varphi_{j'k}(\mathbf{x}), 1 \leq j' \leq m)$ is sorted in descending order, and d is a hyperparameter, that is fixed to .998. A similar strategy was employed in [11] for training. The weights $\phi_{jk}(\mathbf{x})$ are treated as fixed by the model during training.

A pictorial representation of the implemented model is shown in Figure 1. The image \mathbf{x} is fed as input to the inference network $g(\mathbf{x})$. The parameters of the distribution $q(\mathbf{z}|\mathbf{x}, \mathbf{y})$ are computed from the output of the network using equation (11). The gradient of the KL-divergence between $q(\mathbf{z}|\mathbf{x}, \mathbf{y})$ and $p(\mathbf{z}|\mathbf{x})$ is computed using (12) and backpropagated through the inference network. A sample from the continuous relaxation of $q(\mathbf{z}|\mathbf{x}, \mathbf{y})$ is obtained using (14), which is then fed to the classification network along with $\phi_{jk}(\mathbf{x})$. The gradient of the network is computed with respect to the relaxed sample and backpropagated.

3. Evaluation

We evaluate the model on the popular VOC 2012 [5] dataset. The dataset consists of 20 different classes of objects, with high intra-class variation. The task is to segment out an object, if it belongs to one of the 20 classes. Anything other than the 20 objects in the image, is classified as background.

We follow the experimental setup of [24]. In particular, we downloaded approximately 260,000 images of objects belonging to the 20 classes from the Imagenet database [27]. The exact classes of Imagenet used are mentioned in the supplementary section. The downloaded dataset is highly unbalanced, with the 'dog' category having at least 50 times as many images as the category 'potted plant'. We trained the inference network g on this dataset, while ensuring that each class is sampled equal number of times.

3.1. Network architecture

We used the Pytorch framework ¹ for training our network. We downloaded the pretrained VGG16 network (trained on Imagenet for classification) from torchvision ². The fully-connected layers and the last pooling layer were removed from the network and all the other layers of the network were frozen with the pretrained weights. The input images were scaled to 224×224 for training. The output segmentation masks are of size 56×56 . The exact architecture of the inference network g used in our work is shown in Figure 2.

¹<https://github.com/pytorch/pytorch>

²<https://github.com/pytorch/vision/tree/master/torchvision>

class	MIL+ILP [24]	EM-Adapt [21]	CCNN [22]	SEC [11]	STC [37]	Ours
background	77.2	67.2	68.5	82.4	84.5	84.75
aeroplane	37.3	29.2	25.5	62.9	68.0	72.36
bike	18.4	17.6	17.0	26.4	19.5	25.2
bird	25.4	28.6	25.4	61.6	60.5	64.1
boat	28.2	22.2	20.2	27.6	42.5	29.6
bottle	31.9	29.6	26.3	38.1	44.8	53.6
bus	41.6	47.0	46.8	66.6	68.4	53.1
car	48.1	44.0	47.1	62.7	64.0	62.9
cat	50.7	44.2	48.0	75.2	64.8	70.5
chair	12.7	14.6	15.8	22.1	14.5	8.7
cow	53.5	45.7	35.1	53.5	52.0	51.7
diningtable	14.6	24.9	21.0	28.3	22.8	27.0
dog	50.9	41.0	44.5	65.8	58.0	58.2
horse	44.1	34.8	34.5	57.8	55.3	58.4
motorbike	39.2	41.6	46.2	62.3	57.8	46.2
person	37.9	32.1	40.7	62.3	60.5	60.7
plant	28.3	30.4	24.8	32.5	40.6	37.3
sheep	44.0	36.3	37.4	62.6	56.7	66.9
sofa	19.6	24.0	22.2	32.1	23.0	34.1
train	37.6	38.1	38.8	45.4	57.1	40.8
tvmonitor	35.0	31.6	36.9	45.3	31.2	51.6
mean	36.6	33.8	35.3	50.7	49.8	50.4

Table 1: Results on PASCAL VOC 2012 (mIoU in %) *val* set for weakly supervised segmentation.

3.2. Results

In Table 1, we compare the proposed model with other models that were trained solely using image-level annotations, on the validation set of VOC 2012. Among the compared models, the models that employ saliency masks (SEC [11] and STC [37]) have drastically improved performance, as compared to other models. More importantly, the proposed model is able to achieve comparable performance without employing saliency masks. The qualitative results are shown in Figure 2.

4. Discussion

While there have been several papers that posed the problem of semantic segmentation as inference in a graphical model [7, 32, 15, 26, 33, 10, 13, 40], there have been relatively few papers that have achieved the same for weakly supervised semantic segmentation [35, 34]. To our knowledge, this is the first attempt to cast weakly supervised segmentation as learning in a graphical model and utilize CNNs



Table 2: Examples of predicted segmentation masks. The middle row is the ground truth.

for training the graphical model. Graphical modeling is a natural way of incorporating our prior understanding about the data into the model. The fact, that it is also capable

of achieving performance comparable to other architectures that utilize saliency map, suggests that this is the correct direction to proceed.

References

- [1] A. Bearman, O. Russakovsky, V. Ferrari, and L. Fei-Fei. Whats the point: Semantic segmentation with point supervision. In *European Conference on Computer Vision*, pages 549–565. Springer, 2016.
- [2] L.-C. Chen, G. Papandreou, I. Kokkinos, K. Murphy, and A. L. Yuille. Semantic image segmentation with deep convolutional nets and fully connected CRFs. *arXiv preprint arXiv:1412.7062*, 2014.
- [3] L.-C. Chen, G. Papandreou, I. Kokkinos, K. Murphy, and A. L. Yuille. Deeplab: Semantic image segmentation with deep convolutional nets, atrous convolution, and fully connected CRFs. *arXiv preprint arXiv:1606.00915*, 2016.
- [4] J. Dai, K. He, and J. Sun. Boxesup: Exploiting bounding boxes to supervise convolutional networks for semantic segmentation. In *Proceedings of the IEEE International Conference on Computer Vision*, pages 1635–1643, 2015.
- [5] M. Everingham, L. Van Gool, C. K. I. Williams, J. Winn, and A. Zisserman. The PASCAL Visual Object Classes Challenge 2012 (VOC2012) Results. <http://www.pascal-network.org/challenges/VOC/voc2012/workshop/index.html>.
- [6] R. Girshick, J. Donahue, T. Darrell, and J. Malik. Rich feature hierarchies for accurate object detection and semantic segmentation. In *Proceedings of the IEEE conference on Computer Vision and Pattern Recognition*, pages 580–587, 2014.
- [7] X. He, R. S. Zemel, and M. Á. Carreira-Perpiñán. Multiscale conditional random fields for image labeling. In *Proceedings of the 2004 IEEE computer society conference on Computer Vision and Pattern Recognition, 2004*, volume 2, pages II–II. IEEE, 2004.
- [8] E. Jang, S. Gu, and B. Poole. Categorical reparameterization with gumbel-softmax. *arXiv preprint arXiv:1611.01144*, 2016.
- [9] D. P. Kingma and M. Welling. Auto-encoding variational bayes. *arXiv preprint arXiv:1312.6114*, 2013.
- [10] P. Kohli, P. H. Torr, et al. Robust higher order potentials for enforcing label consistency. *International Journal of Computer Vision*, 82(3):302–324, 2009.
- [11] A. Kolesnikov and C. H. Lampert. Seed, expand and constrain: Three principles for weakly-supervised image segmentation. In *European Conference on Computer Vision*, pages 695–711. Springer, 2016.
- [12] P. Kraehenbuehl and V. Koltun. Parameter learning and convergent inference for dense random fields. In *Proceedings of The 30th International Conference on Machine Learning*, pages 513–521, 2013.
- [13] P. Krähenbühl and V. Koltun. Efficient inference in fully connected CRFs with Gaussian edge potentials. In J. Shawe-Taylor, R. S. Zemel, P. L. Bartlett, F. Pereira, and K. Q. Weinberger, editors, *Advances in Neural Information Processing Systems 24*, pages 109–117. Curran Associates, Inc., 2011.
- [14] A. Krizhevsky, I. Sutskever, and G. E. Hinton. Imagenet classification with deep convolutional neural networks. In *Advances in Neural Information Processing Systems*, pages 1097–1105, 2012.
- [15] S. Kumar and M. Hebert. A hierarchical field framework for unified context-based classification. In *Tenth IEEE International Conference on Computer Vision, 2005. ICCV 2005.*, volume 2, pages 1284–1291. IEEE, 2005.
- [16] J. Lafferty, A. McCallum, and F. Pereira. Conditional random fields: Probabilistic models for segmenting and labeling sequence data. In *Proceedings of International Conference on Machine Learning (ICML)*, pages 282–289, 2001.
- [17] V. Lempitsky, P. Kohli, C. Rother, and T. Sharp. Image segmentation with a bounding box prior. In *IEEE 12th International Conference on Computer Vision, 2009*, pages 277–284. IEEE, 2009.
- [18] J. Long, E. Shelhamer, and T. Darrell. Fully convolutional networks for semantic segmentation. In *Proceedings of the IEEE Conference on Computer Vision and Pattern Recognition*, pages 3431–3440, 2015.
- [19] C. J. Maddison, A. Mnih, and Y. W. Teh. The concrete distribution: A continuous relaxation of discrete random variables. *arXiv preprint arXiv:1611.00712*, 2016.
- [20] H. Noh, S. Hong, and B. Han. Learning deconvolution network for semantic segmentation. In *Proceedings of the IEEE International Conference on Computer Vision*, pages 1520–1528, 2015.
- [21] G. Papandreou, L.-C. Chen, K. Murphy, and A. L. Yuille. Weakly-and semi-supervised learning of a dcnn for semantic image segmentation. *arXiv preprint arXiv:1502.02734*, 2015.
- [22] D. Pathak, P. Krahenbuhl, and T. Darrell. Constrained convolutional neural networks for weakly supervised segmentation. In *Proceedings of the IEEE International Conference on Computer Vision*, pages 1796–1804, 2015.
- [23] D. Pathak, E. Shelhamer, J. Long, and T. Darrell. Fully convolutional multi-class multiple instance learning. *arXiv preprint arXiv:1412.7144*, 2014.
- [24] P. O. Pinheiro and R. Collobert. From image-level to pixel-level labeling with convolutional networks. In *Proceedings of the IEEE Conference on Computer Vision and Pattern Recognition*, pages 1713–1721, 2015.
- [25] A. PVS and G. Karthik. Part-of-speech tagging and chunking using conditional random fields and transformation based learning. *Shallow Parsing for South Asian Languages*, 21, 2007.
- [26] A. Rabinovich, A. Vedaldi, C. Galleguillos, E. Wiewiora, and S. Belongie. Objects in context. In *IEEE 11th international conference on Computer vision, 2007. ICCV 2007.*, pages 1–8. IEEE, 2007.
- [27] O. Russakovsky, J. Deng, H. Su, J. Krause, S. Satheesh, S. Ma, Z. Huang, A. Karpathy, A. Khosla, M. Bernstein, A. C. Berg, and L. Fei-Fei. ImageNet Large Scale Visual Recognition Challenge. *International Journal of Computer Vision (IJCV)*, 115(3):211–252, 2015.
- [28] F. Saleh, M. S. A. Akbarian, M. Salzmänn, L. Petersson, S. Gould, and J. M. Alvarez. Built-in foreground/background prior for weakly-supervised semantic segmentation. In *European Conference on Computer Vision*, pages 413–432. Springer, 2016.
- [29] A. G. Schwing and R. Urtasun. Fully connected deep structured networks. *arXiv preprint arXiv:1503.02351*, 2015.

- [30] B. Settles. Biomedical named entity recognition using conditional random fields and rich feature sets. In *Proceedings of the International Joint Workshop on Natural Language Processing in Biomedicine and its Applications*, pages 104–107. Association for Computational Linguistics, 2004.
- [31] W. Shimoda and K. Yanai. Distinct class-specific saliency maps for weakly supervised semantic segmentation. In *European Conference on Computer Vision*, pages 218–234. Springer, 2016.
- [32] J. Shotton, J. Winn, C. Rother, and A. Criminisi. Textonboost: Joint appearance, shape and context modeling for multi-class object recognition and segmentation. In *European Conference on Computer Vision*, pages 1–15. Springer, 2006.
- [33] J. Shotton, J. Winn, C. Rother, and A. Criminisi. Textonboost for image understanding: Multi-class object recognition and segmentation by jointly modeling texture, layout, and context. *International Journal of Computer Vision*, 81(1):2–23, 2009.
- [34] A. Vezhnevets, V. Ferrari, and J. M. Buhmann. Weakly supervised semantic segmentation with a multi-image model. In *2011 IEEE International Conference on Computer Vision (ICCV)*, pages 643–650. IEEE, 2011.
- [35] A. Vezhnevets, V. Ferrari, and J. M. Buhmann. Weakly supervised structured output learning for semantic segmentation. In *2012 IEEE Conference on Computer Vision and Pattern Recognition*, pages 845–852. IEEE, 2012.
- [36] Y. Wei, X. Liang, Y. Chen, Z. Jie, Y. Xiao, Y. Zhao, and S. Yan. Learning to segment with image-level annotations. *Pattern Recognition*, 59:234–244, 2016.
- [37] Y. Wei, X. Liang, Y. Chen, X. Shen, M.-M. Cheng, J. Feng, Y. Zhao, and S. Yan. Stc: A simple to complex framework for weakly-supervised semantic segmentation. *IEEE Transactions on Pattern Analysis and Machine Intelligence*, 2016.
- [38] J. Xu, A. G. Schwing, and R. Urtasun. Tell me what you see and I will show you where it is. In *Proceedings of the IEEE Conference on Computer Vision and Pattern Recognition*, pages 3190–3197, 2014.
- [39] J. Xu, A. G. Schwing, and R. Urtasun. Learning to segment under various forms of weak supervision. In *The IEEE Conference on Computer Vision and Pattern Recognition (CVPR)*, June 2015.
- [40] J. Yao, S. Fidler, and R. Urtasun. Describing the scene as a whole: Joint object detection, scene classification and semantic segmentation. In *2012 IEEE Conference on Computer Vision and Pattern Recognition (CVPR)*, pages 702–709. IEEE, 2012.
- [41] F. Yu and V. Koltun. Multi-scale context aggregation by dilated convolutions. *arXiv preprint arXiv:1511.07122*, 2015.
- [42] S. Zheng, S. Jayasumana, B. Romera-Paredes, V. Vineet, Z. Su, D. Du, C. Huang, and P. H. Torr. Conditional random fields as recurrent neural networks. In *Proceedings of the IEEE International Conference on Computer Vision*, pages 1529–1537, 2015.